SCIENCE CHINA
Mathematics

• ARTICLES •

Science China Mathematics Manuscript for review

A direct finite element method for elliptic interface problems

Jun Hu[1] & Limin Ma[2,*]

[1]*LMAM and School of Mathematical Sciences, Peking University, Beijing* 100871*, People's Republic of China;*
[2]*School of Mathematics and Statistics, Wuhan University, Wuhan* 430072*, People's Republic of China*

*Email: hujun@math.pku.edu.cn *, limin18@whu.edu.cn* †

Abstract In this paper, a direct finite element method is proposed for solving interface problems on simple unfitted meshes. The fact that the two interface conditions form a $H^{\frac{1}{2}}(\Gamma) \times H^{-\frac{1}{2}}(\Gamma)$ pair leads to a simple and direct weak formulation with an integral term for the mutual interaction over the interface, and the well-posedness of this weak formulation is proved. Based on this formulation, a direct finite element method is proposed to solve the problem on two adjacent subdomains separated by the interface by conforming finite element and conforming mixed finite element, respectively. The well-posedness and an optimal a priori analysis are proved for this direct finite element method under some reasonable assumptions. A simple lowest order direct finite element method by using the linear element method and the lowest order Raviart-Thomas element method is proposed and analyzed to admit the optimal a priori error estimate by verifying the aforementioned assumptions. Numerical tests are also conducted to verify the theoretical results and the effectiveness of the direct finite element method.

Keywords unfitted finite element method, interface problem, a priori analysis

MSC(2020) 65N30

Science China Mathematics Manuscript for review

1 Introduction

Consider the following elliptic interface problem

$$-\nabla \cdot (\beta \nabla u) = f \qquad \text{in } \Omega = \Omega^+ \cup \Omega^-, \tag{1.1}$$

$$[u] = 0, \quad [\beta \nabla u \cdot \boldsymbol{n}] = 0 \qquad \text{across } \Gamma, \tag{1.2}$$

$$u = g, \qquad \text{on } \partial\Omega, \tag{1.3}$$

where $\Omega \subset \mathbb{R}^2$ is a bounded Lipschitz domain, $f \in L^2(\Omega)$, $g \in H^{\frac{1}{2}}(\partial\Omega)$, $\Gamma = \partial\Omega^+ \cap \partial\Omega^-$ is a Lipschitz interface that divides Ω into two nonintersecting subdomains Ω^+ and Ω^-. Here $\boldsymbol{n}$ is the unit outer normal

* Corresponding author
*The first author is supported by NSFC project 12288101.
†The second author is supported by NSFC project 12301523 and the Fundamental Research Funds for the Central Universities 413000117.

to Ω^-, and $[v]|_\Gamma = v|_{\Omega^+} - v|_{\Omega^-}$ stands for the jump of a function v across the interface Γ. Assume that the diffusion coefficient β is piecewise constant:

$$\beta = \begin{cases} \beta^+, & (x,y) \in \Omega^+ \\ \beta^-, & (x,y) \in \Omega^- \end{cases}, \quad \text{with} \quad \min\{\beta^+, \beta^-\} > 0.$$

Interface problems with discontinuous coefficients are often encountered in material sciences and fluid dynamics, such as the porous media equations in oil reservoirs. There are extensive studies in the literature on the numerical solutions of interface problems. The numerical methods on body fitted meshes are widely studied, see [1,3,12,17,20,29] for instance. For arbitrarily shaped interface, optimal or nearly optimal convergence rate can be achieved if body-fitted finite element meshes are used in [1,12]. However, it is usually a nontrivial and time-consuming task to generate body-fitted meshes, especially when solving problems with a moving interface or problems in three dimensions.

To avoid the generation of meshes fitting the moving interfaces, an alternative choice for interface problems is to use an unfitted mesh, where the elements are allowed to cross the interface. Various unfitted finite element methods have been proposed in the literature for interface problems. Babuška proved the suboptimal convergence for elliptic interface problem on unfitted meshes in [1]. For the immersed finite element methods and virtual element methods [10, 26] on unfitted meshes, the basis functions near interface need to be modified to satisfy the continuity of the solution u and the flux $\beta\frac{\partial u}{\partial \boldsymbol{n}}$, which poses an H^1-continuity of both the solution and the flux. See [11,15,16,21,22] for references. For the cut finite element methods in [6–8,18,23] and the discontinuous Galerkin methods in [9,25,27], the Nitsche's trick is applied to penalize the discontinuity of basis functions and the corresponding flux over the interface in L^2-norm.

In this paper, a brand new weak formulation for interface problems is established by interpreting the two interface conditions (1.2) as the continuity requirements in $H^{\frac{1}{2}}(\Gamma)$ and $H^{-\frac{1}{2}}(\Gamma)$, respectively. A primal formulation solving the solution in $H^1(\Omega^+)$ space and a mixed formulation solving the flux in H(div, Ω^-) space are adopted on the two subdomains separated by the interface, respectively. Meanwhile, the $H^{\frac{1}{2}}(\Gamma) \times H^{-\frac{1}{2}}(\Gamma)$ pair directly forms an interface integration term in both formulations by use of the Green's formula, and acts as the mutual interaction over the interface in a natural way. To be specific, in the new weak formulation, the first interface condition of (1.2) poses a natural boundary condition for the mixed formulation on Ω^-, and the second condition poses a natural boundary condition for the primal formulation on Ω^+. The new weak formulation leads to a symmetric saddle point system, which is proved to be well posed.

Based on the new weak formulation, a direct finite element method (DiFEM for short hereinafter) is proposed on unfitted meshes. The conforming finite element space is employed on the elements with nonempty intersection with Ω^+, and the conforming mixed finite element space is employed on the elements with nonempty intersections with Ω^-. For elements intersecting with the interface, both the conforming finite element space and the mixed finite element space are employed, where the integration of the corresponding basis functions is conducted merely over Ω^+ and Ω^-, respectively. Practically speaking, only the quadrature formula, which is applied for the integration, brings in the consistency error. The well-posedness of the proposed DiFEM and the optimal a priori analysis are analyzed under some reasonable assumptions on the choice of the discrete spaces and the quadrature formula.

A simple lowest order DiFEM is proposed by using the linear element method for the primal formulation and the lowest order Raviart-Thomas element method for the mixed formulation, respectively. A new Raviart-Thomas interpolation is established by modifying the degrees of freedom of the elements intersecting with the interface, which preserves the crucial commuting property to guarantee the classic inf-sup condition. By verifying the aforementioned assumptions, the well-posedness and an optimal a priori analysis for the lowest order direct finite element method are proved.

There are several advantages of the proposed DiFEM. Firstly, the DiFEM can achieve the optimal convergence on unfitted meshes, which reduces the numerous computational cost caused by generating body-fitted meshes, especially in the case with moving interface. Secondly, the corresponding symmetric

positive semidefinite system allows a wide range of standard fast linear solvers to be utilized. Meanwhile, the DiFEM using standard conforming finite element and mixed finite element allows for a straightforward application of standard solvers for these two methods. Thirdly, the DiFEM can be generalized to three dimensions and high order finite elements. Also, the DiFEM can be applied to other elliptic problems with complicate boundary conditions. For example, for the linear elasticity problem with the stress condition on part of the boundary and the displacement condition on the other part, an artificial interface can be designed to use the mixed finite element on the subdomain with the stress boundary condition and the primal finite element on the subdomain with the displacement boundary condition.

The rest of this paper is organized as follows. Later in this section, some necessary notations and preliminaries are introduced. A brand new weak formulation is established in Section 2.1. The DiFEM is proposed in Section 2.2 with the well-posedness and the optimal convergence proved under some assumptions. In Section 3, a simple lowest order DiFEM is proposed with the optimal a priori analysis analyzed in Section 4. Some numerical experiments are presented in Section 5 to justify our theoretical results and the effectiveness of the proposed method.

Given a nonnegative integer k and a bounded region $G \subset \mathbb{R}^2$, let $H^k(G,\mathbb{R})$, $\|\cdot\|_{k,G}$, $|\cdot|_{k,G}$ and $(\cdot,\cdot)_G$ denote the usual Sobolev spaces, norm, and semi-norm, and the standard L^2 inner product over region G, respectively. For any curve C, let $\langle\cdot,\cdot\rangle_C$ be the duality between $H^{\frac{1}{2}}(C)$ and $H^{-\frac{1}{2}}(C)$, and reduce to the integration when the functions are piecewise polynomials. Let

$$H^k(\Omega_1 \cup \Omega_2) = \{u : u|_{\Omega_1} \in H^k(\Omega_1), \quad u|_{\Omega_2} \in H^k(\Omega_2)\}.$$

For any given function v on Ω, add a superscript '+' or '-' to represent the restriction of v to Ω^+ or Ω^-, respectively, that is $v^+ = v|_{\Omega^+}$, $v^- = v|_{\Omega^-}$. Suppose that Ω is a convex polygonal domain in $\mathbb{R}^2$. For a triangulation $\mathcal{T}_h$ of domain Ω, let $|K|$ and h_K be the area and the diameter of an element $K \in \mathcal{T}_h$, respectively, and $h = \max_{K\in\mathcal{T}_h} h_K$. For each element $K \in \mathcal{T}_h$, define

$$K^+ = K \cap \Omega^+, \qquad K^- = K \cap \Omega^-.$$

For $K \subset \mathbb{R}^2$ and $r \in \mathbb{Z}^+$, let $P_r(K,\mathbb{R})$ be the space of all polynomials of degree not greater than r on K. Throughout the paper, a positive constant independent of the mesh size is denoted by C, which refers to different values at different places. For ease of presentation, we shall use the symbol $A \lesssim B$ to denote that $A \leqslant CB$.

2 Direct Finite Element Method for interface problem

To present the direct finite element for the interface problem (1.1), we first introduce a new weak formulation and analyze its well-posedness in this section.

2.1 A new weak formulation of the interface problem

Define the spaces on Ω^+

$$V_g^+ = \{u^+ \in H^1(\Omega^+), u^+ = g \text{ on } \partial\Omega \cap \partial\Omega^+\}, \quad V^+ = \{u^+ \in H^1(\Omega^+), u^+ = 0 \text{ on } \partial\Omega \cap \partial\Omega^+\},$$

and two Sobolev spaces on Ω^-

$$V^- = L^2(\Omega^-), \quad Q^- = \{\tau^- \in L^2(\Omega^-) : \nabla\cdot\tau^- \in L^2(\Omega^-)\}.$$

Let $\sigma^+ = \beta^+\nabla\cdot u^+$ on the region Ω^+ and $\sigma^- = \beta^-\nabla\cdot u^-$ on the region Ω^-. The primal formulation is adopted for the second order elliptic equation (1.1) on Ω^+, that is for any $v^+ \in V^+$,

$$(\beta^+\nabla u^+, \nabla v^+)_{\Omega^+} = (f^+, v^+)_{\Omega^+} - \langle\beta^+\frac{\partial u^+}{\partial \boldsymbol{n}}, v^+\rangle_\Gamma = (f^+, v^+)_{\Omega^+} - \langle\sigma^+\cdot\boldsymbol{n}, v^+\rangle_\Gamma, \tag{2.1}$$

where $\boldsymbol{n}$ is the unit normal pointing from Ω^- to Ω^+. The mixed formulation for the second order elliptic equation (1.1) on Ω^- reads

$$\begin{cases} \frac{1}{\beta^-}(\sigma^-,\tau^-)_{\Omega^-}+(u^-,\nabla\cdot\tau^-)_{\Omega^-}=\langle u^-,\tau^-\cdot\boldsymbol{n}\rangle_\Gamma+\langle g,\tau^-\cdot\boldsymbol{n}\rangle_{\Gamma_b}, & \forall\tau^-\in Q^- \\ (\nabla\cdot\sigma^-,v^-)_{\Omega^-}=-(f^-,v^-)_{\Omega^-}, & \forall v^-\in V^-, \end{cases} \tag{2.2}$$

where $\Gamma_b=\partial\Omega\cap\partial\Omega^-$. Note that $v^+|_\Gamma\in H^{\frac{1}{2}}(\Gamma)$ for any $v^+\in V^+$ and $\tau^-\cdot\boldsymbol{n}\in H^{-\frac{1}{2}}(\Gamma)$ for any $\tau^-\in Q^-$. The two interface conditions on $u\in H^1(\Omega^+\cup\Omega^-)$ and $\sigma\cdot\boldsymbol{n}$ with $\sigma\in\mathrm{H}(\mathrm{div},\Omega^+\cup\Omega^-)$ forms an $H^{\frac{1}{2}}(\Gamma)\times H^{-\frac{1}{2}}(\Gamma)$ pair for the interface integration term on the right-hand side of both the primal formulation (2.1) and the mixed formulation (2.2). By the interface requirements in (1.1),

$$\sigma^+\cdot\boldsymbol{n}=\sigma^-\cdot\boldsymbol{n},\quad u^+=u^-.$$

Thus, the normal component $\sigma^-\cdot\boldsymbol{n}$ acts as the natural boundary condition for the weak formulation (2.1) on Ω^+, and u^+ acts as the natural boundary condition for the weak formulation (2.2) on Ω^-. We can establish a new formulation which seeks $(\sigma^-,u^-,u^+)\in Q^-\times V^-\times V_g^+$ such that for any $(\tau^-,v^-,v^+)\in Q^-\times V^-\times V^+$,

$$\begin{cases} \frac{1}{\beta^-}(\sigma^-,\tau^-)_{\Omega^-}+(u^-,\nabla\cdot\tau^-)_{\Omega^-}-\langle u^+,\tau^-\cdot\boldsymbol{n}\rangle_\Gamma=\langle g,\tau^-\cdot\boldsymbol{n}\rangle_{\Gamma_b}, \\ (\nabla\cdot\sigma^-,v^-)_{\Omega^-}=-(f^-,v^-)_{\Omega^-}, \\ -\langle\sigma^-\cdot\boldsymbol{n},v^+\rangle_\Gamma-(\beta^+\nabla u^+,\nabla v^+)_{\Omega^+}=-(f^+,v^+)_{\Omega^+}, \end{cases} \tag{2.3}$$

which is a symmetric saddle point system. It can be rewritten as an equivalent saddle point system

$$\begin{cases} a(\sigma^-,u^+;\tau^-,v^+)+b(u^-;\tau^-,v^+)=(f^+,v^+)_{\Omega^+}+\langle g,\tau^-\cdot\boldsymbol{n}\rangle_{\Gamma_b} \\ b(v^-;\sigma^-,u^+)=(f^-,v^-)_{\Omega^-}, \end{cases} \tag{2.4}$$

where the bilinear forms

$$\begin{aligned} a(\sigma^-,u^+;\tau^-,v^+)=&\frac{1}{\beta^-}(\sigma^-,\tau^-)_{\Omega^-}+(\beta^+\nabla u^+,\nabla v^+)_{\Omega^+}+\langle\sigma^-\cdot\boldsymbol{n},v^+\rangle_\Gamma-\langle u^+,\tau^-\cdot\boldsymbol{n}\rangle_\Gamma, \\ b(u^-;\tau^-,v^+)=&(\nabla\cdot\tau^-,u^-)_{\Omega^-}. \end{aligned} \tag{2.5}$$

Although (2.3) and (2.4) are equivalent, the compact form (2.4) is not symmetric because of the bilinear form $a(\cdot,\cdot)$ in (2.5). We will analyze the well-posedness of the proposed weak formulation (2.3) in terms of the nonsymmetric compact form (2.4). For any $(\tau^-,v^+)\in Q^-\times V^+$ and $v^-\in V^-$, define the norms

$$|||(\tau^-,v^+)|||_1=\frac{1}{\sqrt{\beta^-}}\|\tau^-\|_{0,\Omega^-}+\|\nabla\cdot\tau^-\|_{0,\Omega^-}+\sqrt{\beta^+}\|\nabla v^+\|_{0,\Omega^+},\quad |||v^-|||_0=\|v^-\|_{0,\Omega^-}. \tag{2.6}$$

Lemma 2.1. *The weak formulation* (2.4) *is well defined, namely, there exists a unique solution* $(\sigma^-,u^-,u^+)\in Q^-\times V^-\times V_g^+$ *of* (2.4) *and*

$$\begin{aligned} |||(\sigma^-,u^+)|||_1\leqslant& C(\frac{1}{\sqrt{\beta^+}}\|f^+\|_{0,\Omega^+}+\max(\sqrt{\beta^-},1)\|g\|_{\frac{1}{2},\Gamma_b}+C_\beta\|f^-\|_{0,\Omega^-}), \\ |||u^-|||_0\leqslant& CC_\beta(\frac{1}{\sqrt{\beta^+}}\|f^+\|_{0,\Omega^+}+\max(\sqrt{\beta^-},1)\|g\|_{\frac{1}{2},\Gamma_b}+C_\beta\|f\|_{0,\Omega^-}), \end{aligned}$$

where constant C_β *is defined in* (2.8) *and positive constant* C *is independent of* β^+ *and* β^-.

Proof. By the definition of the norms in (2.6), the two bilinear forms $a(\sigma^-,u^+;\tau^-,v^+)$ and $b(u^-;\tau^-,v^+)$ are continuous. To be specific, there exists a positive constant C such that

$$\begin{aligned} |a(\sigma^-,u^+;\tau^-,v^+)|\leqslant& C\max(\sqrt{\beta^-/\beta^+},1)\,|||\,(\sigma^-,u^+)\,|||_1\,|||(\tau^-,v^+)|||_1, \\ |b(u^-;\tau^-,v^+)|\leqslant& |||\,(\tau^-,v^+)\,|||_1\,|||u^-|||_0, \end{aligned}$$

where constant C is independent of β^+ and β^-. Define the kernel space of $Q^- \times V^-$ by

$$Z = \{(\tau^-, v^+) \in Q^- \times V^- : (\nabla\cdot \tau^-, v^-)_{\Omega^-} = 0, \quad \forall v^- \in V^-\}.$$

Note that $\nabla\cdot \tau^- = 0$ for any $(\tau^-, v^+) \in Z$, which indicates that the bilinear form $a(\sigma^-, u^+; \tau^-, v^+)$ is coercive, namely,

$$a(\tau^-, v^+; \tau^-, v^+) = \frac{1}{\beta^-}\|\tau^-\|^2_{0,\Omega^-} + \beta^+\|\nabla v^+\|^2_{0,\Omega^+} \geqslant \frac{1}{2}\,|||\,(\tau^-, v^+)|||^2_1, \quad \forall(\tau^-, v^+) \in Z. \tag{2.7}$$

For any $v^- \in V^-$, there exists $\tau^- \in Q^-$ such that $\nabla\cdot \tau^- = v^-$ and $\|\nabla\cdot \tau^-\|_{0,\Omega^-} + \|\tau^-\|_{0,\Omega^-} \leqslant C\|v^-\|_{0,\Omega^-}$. By the definition of $b(u^-; \tau^-, v^+)$, the inf-sup condition below holds

$$\inf_{0\neq v^-\in V^-}\sup_{(\tau^-,v^+)\in Q^-\times V^+}\frac{b(v^-;\tau^-,v^+)}{|||(\tau^-,v^+)\,|||_1\,|||v^-|||_0} \geqslant \frac{1}{C}\inf_{0\neq v^-\in V^-}\frac{|||v^-|||_0^2}{\max(\frac{1}{\sqrt{\beta^-}},1)\,|||\,v^-|||_0^2} \geqslant \frac{1}{C}\min(\sqrt{\beta^-},1).$$

Let

$$C_\beta = \frac{\max(\sqrt{\beta^-/\beta^+},1)}{\min(\sqrt{\beta^-},1)} = \max(\sqrt{\beta^-},1)\max(\sqrt{\frac{1}{\beta^+}},\sqrt{\frac{1}{\beta^-}}). \tag{2.8}$$

It follows from Theorem 4.2.3 in [4] that

$$\begin{aligned}
|||(\sigma^-, u^+)|||_1 \leqslant& C(\frac{1}{\sqrt{\beta^+}}\|f^+\|_{0,\Omega^+} + \max(\sqrt{\beta^-},1)\|g\|_{\frac{1}{2},\Gamma_b} + C_\beta\|f^-\|_{0,\Omega^-}),\\
|||u^-|||_0 \leqslant& CC_\beta(\frac{1}{\sqrt{\beta^+}}\|f^+\|_{0,\Omega^+} + \max(\sqrt{\beta^-},1)\|g\|_{\frac{1}{2},\Gamma_b} + C_\beta\|f^-\|_{0,\Omega^-}),
\end{aligned}$$

which completes the proof. □

2.2 The direct finite element method

In this section, we propose the DiFEM based on the weak formulation (2.4). Consider finite element spaces

$$V_h^+ \subset V^+, \quad V_h^- \subset V^-, \quad Q_h^- \subset Q^-. \tag{2.9}$$

The DiFEM seeks $(\sigma_h^-, u_h^-, u_h^+) \in Q_h^- \times V_h^- \times V_{g,h}^+$ such that for any $(\tau_h^-, v_h^-, v_h^+) \in Q_h^- \times V_h^- \times V_h^+$,

$$\begin{cases} a(\sigma_h^-, u_h^+; \tau_h^-, v_h^+) + b(u_h^-; \tau_h^-, v_h^+) = (f^+, v_h^+)_{\Omega^+} + \langle g, \tau_h^-\cdot\boldsymbol{n}\rangle_{\Gamma_b} \\ b(v_h^-; \sigma_h^-, u_h^+) = (f^-, v_h^-)_{\Omega^-}, \end{cases} \tag{2.10}$$

where $V_{g,h}^+$ is the corresponding approximation to V_g^+. Notice that the classic conforming element in the $H^1(\Omega^+)$ space is applied to solve the interface problem (1.1) in the subdomain Ω^+ and the conforming mixed element in the H(div) space is applied to solve (1.1) on the subdomain Ω^-. Similar to the weak formulation in (2.3), the discrete formulation (2.10) can be rewritten as a symmetric saddle point system allowing straightforward application of a wide range of standard solvers.

The DiFEM is conforming in the sense that discrete spaces satisfy (2.9), and the linear and bilinear forms used in the DiFEM (2.10) are identical to those of the original weak formulation (2.4). Practically, quadrature schemes are necessary for the computation of both integrals over subdomains Ω^- or Ω^+ and integrals along the interface Γ or the boundary Γ_b. Consider a general quadrature scheme of integrals for $\phi \in H^{1+\varepsilon}(K)$ with $\varepsilon > 0$,

$$\int_{K\cap\Omega^s}\phi(x)\,\mathrm{d}x \sim \sum_{i=1}^{\ell_K^s}\omega_{i,K}^s\phi(x_{i,K}^s), \quad \int_{K\cap C}\phi(x)\,\mathrm{d}x \sim \sum_{i=1}^{\ell_K^C}\omega_{i,K}^C\phi(x_{i,K}^C), \tag{2.11}$$

where the curve $C = \Gamma$ or Γ_b, $x_{i,K}^s$ and positive $\omega_{i,K}^s$ with $s = +, -$, Γ and Γ_b are the integration points and the corresponding weights, respectively. In order to generalize the quadrature formula for

$\phi \in H^1(K)$, we assume that there exist a positive integer ℓ and some approximations Ω_h^s and C_h to Ω^s and curve $C = \Gamma$ or Γ_b, respectively, such that

$$\int_{K\cap\Omega_h^s} \phi(x)\,\mathrm{dx} = \sum_{i=1}^{\ell_K^s} \omega_{i,K}^s \phi(x_{i,K}^s), \quad \int_{K\cap C_h} \phi(x)\,\mathrm{dx} = \sum_{i=1}^{\ell_K^C} \omega_{i,K}^C \phi(x_{i,K}^C), \qquad \forall \phi(x) \in P_\ell(K,\mathbb{R}).$$

The integrations over Ω_h^s and C_h are introduced to avoid using the value of functions at integration points, which requires a relatively higher regularity. This assumption is posed here only for the well-posedness of numerical integrations when $\sigma^-|_K \in H^k(K)$ with $k = 1$, and is not necessary if $\sigma^-|_K \in H^k(K)$ with $k > 1$. Define the discrete L^2 inner product and duality between $H^{\frac{1}{2}}(C)$ and $H^{-\frac{1}{2}}(C)$ by

$$(w,v)_{\Omega^s,h} := \sum_{K\cap\Omega^s\neq\emptyset} (w,v)_{K\cap\Omega_h^s}, \qquad \langle w,v\rangle_{C,h} := \sum_{K\cap C\neq\emptyset} \langle w,v\rangle_{K\cap C_h},$$

and $\|w^s\|_{\Omega^s,h} = \sqrt{(w^s,w^s)_{\Omega^s,h}}$, where $s = +$ or $-$. Here, the duality $\langle w,v\rangle_{C,h}$ reduces to the integration if both functions are piecewise polynomials. The linear system of the DiFEM (2.10) equipped with the integration quadrature formula (2.11) can be written as

$$\begin{cases} a_h(\sigma_h^-,u_h^+;\tau_h^-,v_h^+) + b_h(u_h^-;\tau_h^-,v_h^+) = (f^+,v_h^+)_{\Omega^+,h} + \langle g,\tau_h^-\cdot\boldsymbol{n}\rangle_{\Gamma_b,h} \\ b_h(v_h^-;\sigma_h^-,u_h^+) = (f^-,v_h^-)_{\Omega^-,h}, \end{cases} \tag{2.12}$$

where the bilinear forms

$$\begin{aligned} a_h(\sigma_h^-,u_h^+;\tau_h^-,v_h^+) =& \frac{1}{\beta^-}(\sigma_h^-,\tau_h^-)_{\Omega^-,h} + (\beta^+\nabla u_h^+,\nabla v_h^+)_{\Omega^+,h} + \langle\sigma_h^-\cdot\boldsymbol{n},v_h^+\rangle_{\Gamma,h} - \langle\tau_h^-\cdot\boldsymbol{n},u_h^+\rangle_{\Gamma,h}, \\ b_h(u_h^-;\tau_h^-,v_h^+) =& (\nabla\cdot\tau_h^-,u_h^-)_{\Omega^-,h}. \end{aligned} \tag{2.13}$$

Various quadrature formulas could be used for approximating the bilinear forms on the left-hand sides and the linear forms on the right-hand sides of (2.10), which result in different discrete forms (2.12). It is the application of quadrature formulas that leads to the consistency error of the corresponding DiFEM (2.12).

Assumption 2.2.

1. *For given quadrature formula, $|||\cdot|||_{1,h}$ and $|||\cdot|||_{0,h}$ are norms on $Q_h^-\times V_h^+$ and V_h^-, respectively,*

$$|||(\tau_h^-,v_h^+)|||_{1,h}^2 = \frac{1}{\beta^-}\|\tau_h^-\|_{\Omega^-,h}^2 + \|\Pi_h\nabla\cdot\tau_h^-\|_{\Omega^-,h}^2 + \beta^+\|\nabla v_h^+\|_{\Omega^+,h}^2 \quad |||v_h^-|||_{0,h} = \|v_h^-\|_{\Omega^-,h}, \tag{2.14}$$

where Π_h is the L^2-projection onto V_h^-, namely,

$$(\Pi_h w,v_h^-)_{\Omega^-,h} = (w,v_h^-)_{\Omega^-,h}, \quad \forall v_h^-\in V_h^-,$$

and $\|w_h\|_{\Omega^s,h} = \sqrt{(w_h,w_h)_{\Omega^s,h}}$ with $s = +,\ -$.

2. *The bilinear forms $a_h(\cdot,\cdot)$ and $b_h(\cdot,\cdot)$ are bounded with respect to the norms in (2.14), namely*

$$|a_h(\sigma_h^-,u_h^+;\tau_h^-,v_h^+)| \lesssim |||(\sigma_h^-,u_h^+)|||_{1,h}\,|||(\tau_h^-,v_h^+)|||_{1,h}, \quad |b_h(v_h^-;\sigma_h^-,u_h^+)| \lesssim |||v_h^-|||_{0,h}\,|||(\sigma_h^-,u_h^+)|||_{1,h}. \tag{2.15}$$

3. *The approximate spaces V_h^+, V_h^- and Q_h^- admit the inf-sup conditions. To be specific, there exists positive constant α such that*

$$\inf_{0\neq v_h^-\in V_h^-}\sup_{(\tau_h^-,v_h^+)\in Q_h^-\times V_h^+} \frac{b_h(v_h^-;\tau_h^-,v_h^+)}{|||(\tau_h^-,v_h^+)|||_{1,h}\,|||v_h^-|||_{0,h}} \geqslant \alpha. \tag{2.16}$$

4. There exists the approximation property

$$\inf_{(\tau_h^-,v_h^+)\in Q_h^-\times V_h^+} |||(\sigma^- - \tau_h^-, u^+ - v_h^+)\,|||_{1,h} + \inf_{v_h^-\in V_h^-} |||u^- - v_h^-|||_{0,h} \lesssim h^k, \tag{2.17}$$

provided that $u \in H^{k+1}(\Omega^+\cup\Omega^-)\cap H^1(\Omega)$.

5. The discrete bilinear forms and right-hand terms of (2.12) *satisfy that*

$$\begin{aligned}
&\sup_{(\tau_h^-,v_h^+)\in Q_h^-\times V_h^+} \frac{|a(\sigma^-,u^+;\tau_h^-,v_h^+) - a_h(\sigma^-,u^+;\tau_h^-,v_h^+)|}{|||(\tau_h^-,v_h^+)|||_{1,h}} \lesssim h^k,\\
&\sup_{(\tau_h^-,v_h^+)\in Q_h^-\times V_h^+} \frac{|b(u^-;\tau_h^-,v_h^+) - b_h(u^-;\tau_h^-,v_h^+)|}{|||(\tau_h^-,v_h^+)|||_{1,h}} + \sup_{v_h^-\in V_h^-} \frac{|b(v_h^-;\tau^-,v^+) - b_h(v_h^-;\tau^-,v^+)|}{|||v_h^-|||_{0,h}} \lesssim h^k,\\
&\sup_{(\tau_h^-,v_h^+)\in Q_h^-\times V_h^+} \frac{|(f^+,v_h^+)_{\Omega^+} - (f^+,v_h^+)_{\Omega^+,h}|}{|||(\tau_h^-,v_h^+)|||_{1,h}} + \sup_{v_h^-\in V_h^-} \frac{|(f^-,v_h^-)_{\Omega^-} - (f^-,v_h^-)_{\Omega^-,h}|}{|||v_h^-|||_{0,h}} \lesssim h^k,\\
&\sup_{(\tau_h^-,v_h^+)\in Z_h} \frac{|\langle g,\tau_h^-\cdot\boldsymbol{n}\rangle_{\Gamma_b} - \langle g,\tau_h^-\cdot\boldsymbol{n}\rangle_{\Gamma_b,h}|}{|||(\tau_h^-,v_h^+)|||_{1,h}} \lesssim h^k,
\end{aligned} \tag{2.18}$$

supposed that $u \in H^{k+1}(\Omega^+\cup\Omega^-)\cap H^1(\Omega)$.

Since the weights $\omega_{i,K}^s$ with $s = +$ and $-$ are positive, $(w_h, w_h)_{\Omega^s,h}$ is nonnegative. Quadrature formulas with enough accuracy can guarantee that (2.14) are norms in the corresponding discrete spaces. Note that the boundedness of bilinear forms in (2.15), the discrete inf-sup condition (2.16), and the approximation property (2.17) of discrete spaces are standard requirements for the well-posedness and the convergence of finite element methods, and the last assumption can be easily met if a quadrature formula with high accuracy is adopted.

Remark 2.3. As in the classic theory for mixed finite element methods, the inf-sup condition (2.16) holds if there exists an interpolation operator P_h onto Q_h^- admitting the commuting property

$$\Pi_h\nabla\cdot\tau^- = \nabla\cdot P_h\tau^-. \tag{2.19}$$

For any given $v_h^-\in V_h^+$, there exists $q\in H^1(\Omega^-)$ such that

$$\nabla\cdot\tau^- = v_h^- \quad \text{on } \Omega^-, \quad \text{and} \quad \tau^-\cdot\boldsymbol{n}|_\Gamma = 0$$

with $\|\tau^-\|_{0,\Omega^-} + \|\nabla\cdot\tau^-\|_{0,\Omega^-} \lesssim \|v_h^-\|_{0,\Omega^-}$. Let $\tau_h^- = P_h\tau^-$ and $v_h^+ = 0$. By the commuting property (2.19) of Π_h, it holds that $\Pi_h\nabla\cdot\tau_h^- = \Pi_h\nabla\cdot\tau^-$ and

$$|||(\tau_h^-,v_h^+)|||_{1,h}^2 \lesssim \max(\frac{1}{\beta^-},1)\,|||\,v_h^-|||_{0,h}^2, \tag{2.20}$$

which, together with the fact that $b_h(v_h^-;\tau_h^-,v_h^+) = |||v_h^-|||_{0,h}^2$, leads to the discrete inf-sup condition of the bilinear form $b_h(\cdot,\cdot)$, namely,

$$\inf_{0\neq u_h^-\in V_h^-}\sup_{(\tau_h^-,v_h^+)\in Q_h^-\times V_h^+} \frac{b_h(u_h^-;\tau_h^-,v_h^+)}{|||(\tau_h^-,v_h^+)\,|||_{1,h}\,|||u_h^-|||_{0,h}} \geqslant C\min(\beta^-,1), \qquad \forall u_h^-\in V_h^-.$$

By the classic Babuška–Brezzi theory in [4] and the second Strang lemma in Theorem 4.2.2 of [13], a similar analysis to the one in Lemma 2.1 leads to the following well-posedness and optimal a priori analysis of the DiFEM (2.12) under Assumption 2.2.

Theorem 2.4. *Under Assumption 2.2, the proposed DiFEM* (2.12) *is well defined, namely, there exists a unique solution* $(\sigma_h^-,u_h^-,u_h^+)\in Q_h^-\times V_h^-\times V_{g,h}^+$ *of* (2.12) *and*

$$|||(\sigma_h^-,u_h^+)\,|||_{1,h} + |||\,u_h^-|||_{0,h} \lesssim \|f\|_{0,\Omega}.$$

Moreover, the solution $(\sigma_h^-, u_h^-, u_h^+)$ *admits the optimal convergence*

$$|||(\sigma^- - \sigma_h^-, u^+ - u_h^+)|||_{1,h} + |||\, u^- - u_h^-|||_{0,h} \lesssim h^k, \tag{2.21}$$

provided that $u \in H^{k+1}(\Omega^+ \cup \Omega^-) \cap H^1(\Omega)$.

Proof. Define the discrete kernel space

$$Z_h = \{(\tau_h^-, v_h^+) \in Q_h^- \times V_h^+ : (\nabla\cdot \tau_h^-, v_h^-)_{\Omega^-,h} = 0, \quad \forall v_h^- \in V_h^-\}.$$

For any $(\tau_h^-, v_h^+) \in Z_h\backslash\{0\}$, it holds that $\Pi_h \nabla \cdot \tau_h^- = 0$. By the definition of $a_h(\cdot,\cdot)$ in (2.13),

$$a_h(\tau_h^-, v_h^+; \tau_h^-, v_h^+) = \frac{1}{\beta^-}\|\tau_h^-\|_{\Omega^-,h}^2 + \beta^+\|\nabla v_h^+\|_{\Omega^+,h}^2 = |||(\tau_h^-, v_h^+)|||_{1,h}^2, \tag{2.22}$$

which indicates that $a_h(\cdot,\cdot)$ is coercive in Z_h. A combination of the inf-sup conditions (2.16) of the bilinear form $b_h(\cdot,\cdot)$, the coercivity (2.22) of the bilinear form $a_h(\cdot,\cdot)$, Assumption 2.2, and the classic Babuška–Brezzi theory in [4] proves that the DiFEM (2.12) is well posed.

For any $(\tau_h^-, v_h^+) \in Q_h^- \times V_h^+$ and $w_h^- \in V_h^-$, the inf-sup condition (2.16) of $b_h(\cdot,\cdot)$ indicates that

$$|||(\sigma_h^- - \tau_h^-, u_h^+ - v_h^+)|||_{1,h} \lesssim \frac{|b_h(\sigma^- - \tau_h^-, u^+ - v_h^+; w_h^-)| + |b_h(\sigma^- - \sigma_h^-, u^+ - v_h^+; w_h^-)|}{|||w_h^-|||_{0,h}}. \tag{2.23}$$

By the weak formulation (2.4), the DiFEM (2.12) and the consistency error estimate (2.18) in Assumption 2.2,

$$\begin{aligned}|b_h(\sigma^- - \sigma_h^-, u^+ - v_h^+; w_h^-)| \leqslant& |(f^-, w_h^-)_{\Omega^-} - (f^-, w_h^-)_{\Omega^-,h}| + |b_h(\sigma^-, u^+; w_h^-) - b(\sigma^-, u^+; w_h^-)|\\ \lesssim& h^k\, |||\, w_h^-\, |||_{0,h}\,.\end{aligned}$$

A substitution of this, the boundedness of $b_h(\cdot,\cdot)$ in (2.15) and the approximation property (2.17) in Assumption 2.2 into (2.23) leads to

$$|||(\sigma_h^- - \tau_h^-, u_h^+ - v_h^+)|||_{1,h} \lesssim |||(\sigma - \tau_h^-, u^+ - v_h^+)\, |||_{1,h} + h^k \lesssim h^k,$$

which, together with (2.17), proves

$$|||(\sigma^- - \sigma_h^-, u^+ - u_h^+)|||_{1,h} \lesssim \inf_{(\tau_h^-, v_h^+)\in Q_h^- \times V_h^+} |||(\sigma^- - \tau_h^-, u^+ - v_h^+)\, |||_{1,h} + h^k \lesssim h^k.$$

By the weak formulation (2.4), the DiFEM (2.12) and (2.18) in Assumption 2.2,

$$\begin{aligned}&|b_h(\tau_h^-, v_h^+; u^- - u_h^-)|\\ \leqslant& |(f^+, v_h^+)_{\Omega^+} - (f^+, v_h^+)_{\Omega^+,h}| + |\langle g, \tau_h^-\cdot\boldsymbol{n}\rangle_{\Gamma_b} - \langle g, \tau_h^-\cdot\boldsymbol{n}\rangle_{\Gamma_b,h}| + |a_h(\sigma_h^- - \sigma^-, u_h^+ - u^+; \tau_h^-, v_h^+)|\\ &+ |a_h(\sigma^-, u^+; \tau_h^-, v_h^+) - a(\sigma^-, u^+; \tau_h^-, v_h^+)| + |b(u^-; \tau_h^-, v_h^+) - b_h(u^-; \tau_h^-, v_h^+)| \lesssim h^k\, |||\, (\tau_h^-, v_h^+)|||_{1,h},\end{aligned}$$

where the analysis of the first term on the right-hand side of (2.21) is applied for the second term. Thus, the discrete inf-sup condition of the bilinear form $b_h(\cdot,\cdot)$ in (2.16) indicates that

$$|||u^- - u_h^-|||_{0,h} \lesssim h^k,$$

which completes the proof.

□

3 A simple lowest order DiFEM

In this section, we consider the lowest order finite element method with a particular quadrature formula as an example, and analyze the well-posedness and optimal a priori error estimate under the following assumption.

Assumption 3.1. *Assume that* $\Gamma = \Gamma_1 \cup \cdots \cup \Gamma_k$ *is a curve or the union of several separated curves, where each curve is of class* C^2.

1. *For any element* K, *the interface* Γ *intersects the boundary of* K *at most twice at different edges (including the end points).*
2. *There exists at least one intersecting element with an edge belonging to* Ω^+.

Note that the first assumption holds if the mesh size is small enough to resolve the interface Γ, and it can even be removed if some certain quadrature rules are chosen such that Assumption 2.2 is satisfied. The second assumption always holds if the interface is not a Jordan curve, and also if there exists at least one triangle inside the region enclosed by the Jordan curve, which is true when the mesh size is not too large.

Consider the linear element space and the lowest order Raviart-Thomas element space [24] on a triangulation $\mathcal{T}_h$ as below.

$$
\begin{aligned}
&V_h^+ := V_{\mathrm{P}_1}^+ = \{v_h^+ \in H^1(\Omega^+) : v_h^+|_K \in P_1(K) \text{ for any } K \cap \Omega^+ \neq \emptyset,\ v_h^+ = 0 \text{ on } \partial\Omega\},\\
&V_{g,h}^+ := V_{\mathrm{g},\mathrm{P}_1}^+ = \{v_h^+ \in H^1(\Omega^+) : v_h^+|_K \in P_1(K) \text{ for any } K \cap \Omega^+ \neq \emptyset,\ v_h^+(p) = g(p) \text{ for any vertex } \ p \in \partial\Omega\},\\
&Q_h^- := Q_{\mathrm{RT}}^- = \{\tau_h^- \in L^2(\Omega^-) : \tau_h^-|_K \in \mathrm{RT}(K) \text{ for any } K \cap \Omega^- \neq \emptyset,\ \nabla\cdot\tau_h^- \in L^2(\Omega^-)\},\\
&V_h^- := V_{\mathrm{P}_0}^- = \{v_h^- \in L^2(\Omega^-) : v_h^-|_K \in P_0(K) \text{ for any } K \cap \Omega^- \neq \emptyset\},
\end{aligned}
\tag{3.1}
$$

where the shape function space $\mathrm{RT}(K) := P_0(K) + \boldsymbol{x}P_0(K)$. For any element K intersecting with Γ or Γ_b, let $\Gamma_{K,h}$ be the line segment connecting the two intersects of Γ or Γ_b and ∂K, K_h^+ be the convex hull of the vertices of K in Ω^+ and the endpoints of $\Gamma_{K,h}$, and K_h^- be the remaining part of K. If K is a subset of Ω^+, then $K_h^+ = K$ and $K_h^- = \emptyset$. Similarly, $K_h^- = K$ and $K_h^+ = \emptyset$ if K is a subset of Ω^-. For the quadrature formula in (2.11), let

$$
\ell_K^\Gamma = 1, \quad \omega_{1,K}^\Gamma = |\Gamma_{K,h}|, \quad x_{1,K}^\Gamma = \text{the midpoint of } \Gamma_{K,h}, \tag{3.2}
$$

and choose $\omega_{i,K}^s$ and $x_{i,K}^s$ with $s = +, -$ such that

$$
\int_{K_h^s} \phi(x)\,\mathrm{dx} = \sum_{i=1}^{\ell_K^s} \omega_{i,K}^s \phi(x_{i,K}^s), \quad \forall \phi(x) \in P_2(K_h^s, \mathbb{R}). \tag{3.3}
$$

It shows that $\int_{\Gamma_{K,h}} \phi(x)\,\mathrm{ds} = \omega_{1,K}^\Gamma \phi(x_{1,K}^\Gamma)$ for any linear polynomial $\phi(x)$. The DiFEM (2.12) with discrete spaces (3.1) and quadrature formulas (3.2) and (3.3) is wellposed and admit the optimal convergence as presented in the following theorem.

Theorem 3.2. *If Assumption 3.1 holds, there exists a unique solution* $(\sigma_h^-, u_h^-, u_h^+) \in Q_{\mathrm{RT}}^- \times V_{\mathrm{P}_0}^- \times V_{\mathrm{P}_1}^+$ *of the DiFEM* (2.12) *with discrete spaces* (3.1) *and quadrature formulas* (3.2) *and* (3.3), *satisfying*

$$
|||(\sigma^- - \sigma_h^-, u^+ - u_h^+)|||_{1,h} + |||\, u^- - u_h^-\,|||_{0,h} \lesssim h,
$$

provided that $u \in H^2(\Omega^+ \cup \Omega^-) \cap H^1(\Omega)$.

In the next section, we will focus on the proof of Theorem 3.2 by verifying the requirements in Assumption 2.2 in Lemma 4.1- Lemma 4.3.

4 Well-posedness and optimal convergence of the lowest order method

Lemma 4.1. *The bilinear forms* $a_h(\cdot,\cdot)$ *and* $b_h(\cdot,\cdot)$ *in* (2.13) *with the particular quadrature formulas in* (3.2) *and* (3.3) *are bounded with respect to the norms in* (2.14).

Proof. We first prove that $\|\nabla v_h^+\|_{\Omega^+,h}$ and $\|\tau_h^-\|_{\Omega^-,h}$ are norms in $V_{\mathrm{P}_1}^+$ and Q_{RT}^-, respectively. It is easy to verify the semipositive property, the linearity and the triangle inequality by the definition of

both $\|\nabla v_h^+\|_{\Omega^+,h}$ and $\|v_h^+\|_{\Omega^-,h}$. If $\|\nabla v_h^+\|_{\Omega^+,h}=0$, by the definition of $\|\cdot\|_{\Omega^+,h}$ in (3.3) and the fact that ∇v_h^+ is piecewise constant, it holds that

$$\sum_{K\cap\Omega^+\neq\emptyset}\|\nabla v_h^+\|_{0,K_h^+}=\|\nabla v_h^+\|_{\Omega^+,h}=0,$$

which implies that $v_h^+=0$ since $v_h^+\in V_{\mathrm{P}_1}^+$. Thus, $\|\nabla v_h^+\|_{\Omega^+,h}$ is a norm on $V_{\mathrm{P}_1}^+$. Similarly, since $\tau_h^-\in Q_{\mathrm{RT}}^-$ is piecewise linear, it follows from (3.3) that if $\|\tau_h^-\|_{\Omega^-,h}=0$,

$$\sum_{K\cap\Omega^-\neq\emptyset}\|\tau_h^-\|_{0,K_h^-}=\|\tau_h^-\|_{\Omega^-,h}=0,$$

which implies that $\tau_h^-=0$. Then, $\|\tau_h^-\|_{\Omega^-,h}$ is a norm on Q_{RT}^-. Furthermore, $|||(\tau_h^-,v_h^+)|||_h$ and $|||v_h^-|||_h$ in (2.14) are norms in $Q_{\mathrm{RT}}^-\times V_{\mathrm{P}_1}^+$ and $V_{\mathrm{P}_0}^-$, respectively.

Note that $v_h^+\in V_{\mathrm{P}_1}^+$ and $\tau_h^-\in Q_{\mathrm{RT}}^-$ are piecewise linear with constant $\tau_h^-\cdot\boldsymbol{n}$ on $\Gamma_{K,h}$ if element K intersects with the interface Γ. By the quadrature formulas (3.2) and (3.3), the bilinear forms in (2.13) can be written in an equivalent way

$$\begin{aligned}a_h(\sigma_h^-,u_h^+;\tau_h^-,v_h^+)&=\sum_{K\in\mathcal{T}_h}\frac{1}{\beta^-}(\sigma_h^-,\tau_h^-)_{K_h^-}+(\nabla u_h^+,\nabla v_h^+)_{K_h^+}+\langle\sigma_h^-\cdot\boldsymbol{n},v_h^+\rangle_{\Gamma_{K,h}}-\langle\tau_h^-\cdot\boldsymbol{n},u_h^+\rangle_{\Gamma_{K,h}},\\ b_h(u_h^-;\tau_h^-,v_h^+)&=\sum_{K\in\mathcal{T}_h}(u_h^-\nabla\cdot,\tau_h^-)_{K_h^-},\end{aligned}\tag{4.1}$$

and the norms in (2.14) can be rewritten as

$$|||(\tau_h^-,v_h^+)|||_h^2=\sum_{K\in\mathcal{T}_h}\frac{1}{\beta^-}\|\tau_h^-\|_{0,K_h^-}^2+\|\nabla\cdot\tau_h^-\|_{0,K_h^-}^2+\beta^+\|\nabla v_h^+\|_{0,K_h^+}^2,\quad |||v_h^-|||_h^2=\sum_{K\in\mathcal{T}_h}\|v_h^-\|_{0,K_h^-}^2.\tag{4.2}$$

By the Cauchy-Schwarz inequality and the inverse trace inequality in [28],

$$\sum_{K\in\mathcal{T}_h}\left|\langle\sigma_h^-\cdot\boldsymbol{n},v_h^+\rangle_{\Gamma_{K,h}}\right|\leqslant\sum_{K\in\mathcal{T}_h}\|h^{\frac12}\sigma_h^-\cdot\boldsymbol{n}\|_{0,\Gamma_{K,h}}\|h^{-\frac12}v_h^+\|_{0,\Gamma_{K,h}}\lesssim\|\sigma_h^-\|_{\Omega^-,h}\|v_h^+\|_{\Omega^+,h}.$$

The boundedness (2.15) of the bilinear forms $a_h(\cdot,\cdot)$ and $b_h(\cdot,\cdot)$ in (4.1) follows from this estimate and the Cauchy-Schwarz inequality, which completes the proof. □

In order to verify the inf-sup condition (2.16) in Assumption 2.2, we first prove the crucial commuting property. According to [12], the problem (1.1) has a unique solution $u\in H^1(\Omega)\cap H^2(\Omega^+\cup\Omega^-)$ assuming $f\in L^2(\Omega)$. Recall that u^+ and u^- are the restrictions of u to Ω^+ and Ω^-, respectively. By the extension theorem for Sobolev spaces, we can extend the continuous $u^+\in H^2(\Omega^+)$ to $\tilde{u}^+\in H^2(\Omega^+\cup\Omega_h^+)$ such that $\tilde{u}^+$ is a continuous function with $\tilde{u}^+|_{\Omega^+}=u^+$ and $\|\tilde{u}^+\|_{0,\Omega_h^+}\lesssim\|u^+\|_{0,\Omega^+}$. Let $\tilde{f}^+=-\nabla\cdot(\beta^+\nabla\tilde{u}^+)$, Then the restriction of $\tilde{f}^+$ equals to f^+ on Ω^+ with $\|\tilde{f}^+\|_{0,\Omega_h^+}\lesssim\|f^+\|_{0,\Omega^+}$. We can also extend u^- and define $\tilde{u}^-$, $\tilde{\sigma}^-$ and $\tilde{f}^-$ in the same way. For the ease of presentation, we will omit the tilde of the all these variables in the analysis below.

Lemma 4.2. *If Assumption 3.1 holds, there exists an interpolation $\Pi_{\mathrm{RT}}^*:Q^-\to Q_{\mathrm{RT}}^-$ admitting the commuting property*

$$\nabla\cdot\Pi_{\mathrm{RT}}^*\tau^-=\Pi_h^0\nabla\cdot\tau^-,\quad\forall\tau^-\in Q^-,\tag{4.3}$$

where the L^2 projection $\Pi_h^0v^-|_K=\Pi_K^0v^-$ for all $K\in\mathcal{T}_h$ with nonempty intersection with Ω^-, and

$$\Pi_K^0v^-=\frac{1}{|K_h^-|}\int_{K_h^-}v^-\,\mathrm{d}x.\tag{4.4}$$

Moreover, it holds that

$$\inf_{(\tau_h^-,v_h^+)\in Q_{\mathrm{RT}}^-\times V_{\mathrm{P}_1}^+}|||(\sigma^--\tau_h^-,u^+-v_h^+)|||_{1,h}+\inf_{v_h^-\in V_{\mathrm{P}_0}^-}|||u^--v_h^-|||_{0,h}\lesssim h,\tag{4.5}$$

provided that $u\in H^2(\Omega^-\cup\Omega^+)\cap H^1(\Omega)$.

Proof. Suppose that there are n_T elements intersecting with the interface Γ with labels $\{K_i\}_{i=1}^{n_T}$, where K_i and K_{i+1} share a common edge. For all the edges of these interface elements, suppose that there are n_c edges intersecting with Γ, n_o edges belonging to Ω^+ and n_i edges belonging to Ω^-, which are labeled by $\{e_i\}_{i=1}^{n_c}$, $\{e_i\}_{i=n_c+1}^{n_c+n_o}$ and $\{e_i\}_{i=n_c+n_o+1}^{n_c+n_o+n_i}$, respectively. For all the other interior elements of Ω^-, denote the edges in Ω^- without intersecting with interface elements by $\{e_i\}_{i=n_c+n_o+n_i+1}^{n_e^-}$. For ease of presentation, let e_1 and e_2 be the edges of element K_1, and intersecting edges e_i and e_{i+1} with $1 \leqslant i \leqslant n_c - 1$ share a common vertex. Figure 1 shows a simple example of these notations.

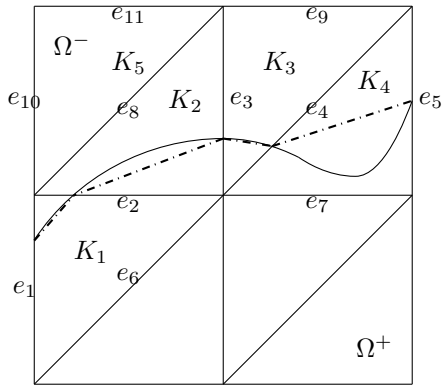

Figure 1 For an interface, which is not a Jordan curve, the elements in Ω_h^- and the corresponding edges are shown with $n_T = 4$, $n_c = 5$, $n_o = 2$, $n_i = 2$ and $n_e^- = 11$.

The degrees of freedom for the Raviart-Thomas element are defined by

$$d_i(\tau_h^-) = \frac{1}{|e_i|}\int_{e_i} \tau_h^- \cdot \boldsymbol{n}_{e_i}\,\mathrm{ds}, \quad 1 \leqslant i \leqslant n_e^-,$$

where $\boldsymbol{n}_{e_i}$ is the normal direction pointing from the element with smaller index to the element with larger index. Denote the corresponding basis function with respect to d_i by $\phi_i(x)$. If e_i is a common edge of elements K_{i_1} and K_{i_1+1}, the basis function

$$\phi_i|_{K_{i_1}} = \frac{|e_i|}{2|K_{i_1}|}(x - p^i_{K_{i_1}}), \quad \phi_i|_{K_{i_1+1}} = -\frac{|e_i|}{2|K_{i_1+1}|}(x - p^i_{K_{i_1+1}}),$$

where p^i_K is the vertex of K not belonging to e_i. Since $\Pi^*_{\mathrm{RT}}\tau^- \in Q^-_{\mathrm{RT}}$, it only remains to determine $d_i(\Pi^*_{\mathrm{RT}}\tau^-)$ for $1 \leqslant i \leqslant n_e^-$.

For $\tau^- \in Q^-$, let $\Pi^*_{\mathrm{RT}}\tau^- \in Q^-_{\mathrm{RT}}$ satisfy that

$$d_i(\Pi^*_{\mathrm{RT}}\tau^-) = d_i(\tau^-), \quad n_c + n_o + 1 \leqslant i \leqslant n_e^-, \tag{4.6}$$

and

$$\sum_{i=1}^{n_c+n_o+n_i} d_i(\Pi^*_{\mathrm{RT}}\tau^-)\Pi^0_{K_j}\nabla\cdot\phi_i(x) = \Pi^0_{K_j}\nabla\cdot\tau^-, \quad \forall 1 \leqslant j \leqslant n_T. \tag{4.7}$$

The definition in (4.6) shows that the interpolation Π^*_{RT} shares the same degrees of freedom with the canonical interpolation of the Raviart-Thomas element on all the interior edges of Ω^-.

Next, we prove that this definition is well posed, namely the linear system (4.7) is solvable. The constraint (4.7) is equivalent to

$$\left[\, A_{n_T\times n_c} \,\middle|\, A_{n_T\times n_o} \,\right] \begin{bmatrix} \vec{d}_{n_c} \\ \vec{d}_{n_o} \end{bmatrix} = \vec{b}_{n_T}, \quad \vec{b}_{n_T} = [b_1, \cdots, b_{n_T}]^T,$$

where $\vec{d}_{n_c} = [d_1(\Pi^*_{\mathrm{RT}}\tau^-), \cdots, d_{n_c}(\Pi^*_{\mathrm{RT}}\tau^-)]^T$, $\vec{d}_{n_o} = [d_{n_c+1}(\Pi^*_{\mathrm{RT}}\tau^-), \cdots, d_{n_c+n_o}(\Pi^*_{\mathrm{RT}}\tau^-)]^T$ and

$$A_{n_T\times n_c} = \begin{bmatrix} a_{1,1} & a_{1,2} & a_{1,3} & \cdots & a_{1,n_c} \\ a_{2,1} & a_{2,2} & a_{2,3} & \cdots & a_{2,n_c} \\ a_{3,1} & a_{3,2} & a_{3,3} & \cdots & a_{3,n_c} \\ \vdots & \vdots & \vdots & \ddots & \vdots \\ a_{n_T-1,1} & a_{n_T-1,2} & a_{n_T-1,3} & \cdots & a_{n_T-1,n_c} \\ a_{n_T,1} & a_{n_T,2} & a_{n_T,3} & \cdots & a_{n_T,n_c} \end{bmatrix}, \quad A_{n_T\times n_o} = \begin{bmatrix} a_{1,n_c+1} & \cdots & a_{1,n_c+n_o} \\ a_{2,n_c+1} & \cdots & a_{2,n_c+n_o} \\ a_{3,n_c+1} & \cdots & a_{3,n_c+n_o} \\ \vdots & \ddots & \vdots \\ a_{n_T-1,n_c+1} & \cdots & a_{n_T-1,n_c+n_o} \\ a_{n_T,n_c+1} & \cdots & a_{n_T,n_c+n_o} \end{bmatrix}$$

with $a_{ij} = \Pi^0_{K_i}\nabla\cdot\phi_j$ and $b_i = \Pi^0_{K_i}\nabla\cdot\tau^- - \sum_{j=n_c+n_o+1}^{n_c+n_o+n_i} d_j(\Pi^*_{\mathrm{RT}}\tau^-)\Pi^0_{K_i}\nabla\cdot\phi_j$. By the definition of $\phi_i(x)$, $a_{ij} = (-1)^{i-j}\frac{|e_j|}{|K_i|}$ is positive if e_j is an edge of K_i, otherwise, $a_{ij} = 0$.

If the interface Γ is not a Jordan curve as shown in Figure 1, e_i and e_{i+1} are two edges of an interface element K_i for $1 \leqslant i \leqslant n_T$ and the number of intersecting edges is larger than the number of intersecting elements, that is $n_c = n_T + 1$. Since $a_{i,i}$ is always nonzero, the coefficient matrix

$$A_{n_T\times n_c} = \begin{bmatrix} a_{1,1} & a_{1,2} & 0 & 0 & \cdots & 0 & 0 \\ 0 & a_{2,2} & a_{2,3} & 0 & \cdots & 0 & 0 \\ 0 & 0 & a_{3,3} & a_{3,4} & \cdots & 0 & 0 \\ \vdots & \vdots & \vdots & \vdots & \ddots & \vdots & \vdots \\ 0 & 0 & 0 & 0 & \cdots & a_{n_T,n_T} & a_{n_T,n_T+1} \end{bmatrix}, \ \mathrm{rank}(A_{n_T\times n_c}) = n_T.$$

It follows that

$$\mathrm{rank}(A_{n_T\times n_c}|A_{n_T\times n_o}) = \mathrm{rank}(A_{n_T\times n_c}) = n_T,$$

which implies the existence of solution for the linear system (4.7) if Γ is not a Jordan curve. Constraints $d_i(\Pi^*_{\mathrm{RT}}\tau^-) = d_i(\tau^-)$ for all $n_c \leqslant i \leqslant n_c + n_o$ are posed to guarantee the uniqueness of the solution of (4.7).

Consider the case that the interface Γ is a Jordan curve as shown in Figure 2. Let e_i and e_{i+1} are

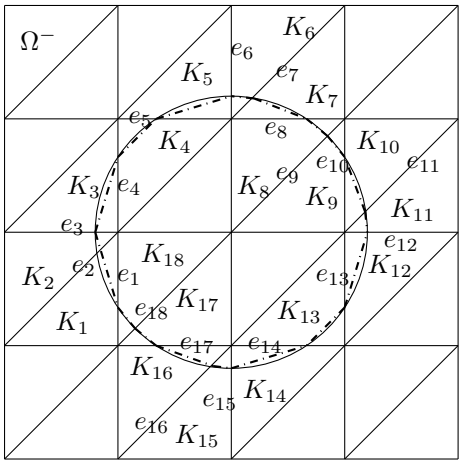

Figure 2 For a Jordan curve, the intersecting elements in Ω^*_h and the intersecting edges are shown with $n_T = 18$, $n_c = 18$, $n_o = 6$, $n_i = 12$ and $n_e^- = 56$.

two edges of an interface element K_i for $1 \leqslant i \leqslant n_T - 1$, and e_1 and e_{n_T} are two edges of an interface element K_{n_T}. Note that the number of intersecting edges equals to the number of intersecting elements,

that is $n_c = n_T$. The coefficient matrix $A_{n_T\times n_c}$ is a square matrix

$$A_{n_T\times n_c} = \begin{bmatrix} a_{1,1} & a_{1,2} & 0 & 0 & \cdots & 0 & 0 & 0 \\ 0 & a_{2,2} & a_{2,3} & 0 & \cdots & 0 & 0 & 0 \\ 0 & 0 & a_{3,3} & a_{3,4} & \cdots & 0 & 0 & 0 \\ \vdots & \vdots & \vdots & \vdots & \ddots & \vdots & \vdots & \vdots \\ 0 & 0 & 0 & 0 & \cdots & 0 & a_{n_T-1,n_T-1} & a_{n_T-1,n_T} \\ a_{n_T,1} & 0 & 0 & 0 & \cdots & 0 & 0 & a_{n_T,n_T} \end{bmatrix}.$$

Multiply the i-th row ($1 \leqslant i \leqslant n_T - 1$) of $A_{n_T\times n_c}$ by $\frac{|K_i|}{|K_{n_T}|}$ and add all these rows to the last row of $A_{n_T\times n_c}$. Then,

$$\operatorname{rank}(A_{n_T\times n_c}) = \operatorname{rank}(\begin{bmatrix} \tilde{a}_{1,1} & \tilde{a}_{1,2} & 0 & 0 & \cdots & 0 & 0 & 0 \\ 0 & \tilde{a}_{2,2} & \tilde{a}_{2,3} & 0 & \cdots & 0 & 0 & 0 \\ 0 & 0 & \tilde{a}_{3,3} & \tilde{a}_{3,4} & \cdots & 0 & 0 & 0 \\ \vdots & \vdots & \vdots & \vdots & \ddots & \vdots & \vdots & \vdots \\ 0 & 0 & 0 & 0 & \cdots & 0 & \tilde{a}_{n_T-1,n_T-1} & \tilde{a}_{n_T-1,n_T} \\ 0 & 0 & 0 & 0 & \cdots & 0 & 0 & 0 \end{bmatrix}),$$

where $\tilde{a}_{i,j} = (-1)^{i-j}\frac{|e_j|}{|K_{n_T}|}$ for $1 \leqslant j \leqslant n_T - 1$, which implies that

$$\operatorname{rank}(A_{n_T\times n_c}) = n_T - 1.$$

Since there exists at least one intersecting element with an edge belonging to Ω^+, we can label this intersecting element by K_{n_T}, the element sharing an edge with K_{n_T} by K_1, and the edge of K_{n_T} belonging to Ω^+ by e_{n_c+1}. Then, constraint (4.7) with $j = n_T$ can be written as

$$d_1(\Pi^*_{\mathrm{RT}}\tau^-)\Pi^0_{K_j}\nabla\cdot\phi_1 + d_{n_c}(\Pi^*_{\mathrm{RT}}\tau^-)\Pi^0_{K_j}\nabla\cdot\phi_{n_c} + d_{n_c+1}(\Pi^*_{\mathrm{RT}}\tau^-)\Pi^0_{K_j}\nabla\cdot\phi_{n_c+1} = \Pi^0_{K_j}\nabla\cdot\tau^-,$$

which indicates that $a_{n_T,n_c+1} = \frac{1}{|K_{n_T}|} \neq 0$. It follows that

$$\operatorname{rank}(A_{n_T\times n_c}|A_{n_T\times n_o}) = n_T,$$

which implies the existence of solution for the linear system (4.7) if Γ is a Jordan curve, and shows the existence of interpolation Π^*_{RT} satisfying (4.6) and (4.7). Then $d_{n_c+1}(\Pi^*_{\mathrm{RT}}\tau^-)$ should be computed by the equation (4.7), and constraints $d_i(\Pi^*_{\mathrm{RT}}\tau^-) = d_i(\tau^-)$ for all $n_c + 2 \leqslant i \leqslant n_c + n_o$ are posed to guarantee the uniqueness of the solution of (4.7).

If the interface is the union of several separated curves, the edges intersecting with the interface can be divided into several classes such that the edges in each class intersect with the same separated curve. Then all the degrees of freedom with respect to edges in the same class can be computed by solving a linear system as discussed above, which complete the proof of the commuting property in (4.3).

Let $\tau^-_h = \Pi_{\mathrm{RT}}\tau^-$ and $v^+_h = \Pi_{\mathrm{P}_1}v^+$ be the canonical interpolation of the Raviart-Thomas element and the linear element, respectively, and $v^-_h = \Pi^0_h$ be the piecewise constant projection. It holds that

$$\|\sigma^- - \tau^-_h\|_{\Omega^-,h} + \|\nabla\cdot(\sigma^- - \tau^-_h)\|_{\Omega^-,h} + \|\nabla(u^+ - v^+_h)\|_{\Omega^+,h} + \|u^- - v^-_h\|_{\Omega^-,h} \lesssim h,$$

which completes the proof of (4.5). □

Lemma 4.3. *Under Assumption 3.1, the consistency error estimate* (2.18) *holds for the DiFEM* (2.12) *with finite element spaces* (3.1) *and quadrature formulas* (3.2) *and* (3.3).

Proof. Recall that K_h^+ is the convex hull of the vertices of K in Ω^+ and the endpoints of $\Gamma_{K,h}$. By the quadrature formula (3.3) and the Bramble-Hilbert lemma, the difference between the L^2 inner product and that by the quadrature formula admits the following estimate

$$|(f^+, v_h^+)_{K_h^+} - (f^+, v_h^+)_{K_h^+,h}| \lesssim h^2 \|f^+\|_{2,K_h^+} \|v_h^+\|_{0,K_h^+}, \quad \forall v_h^+ \in V_{\mathrm{P}_1}^+. \tag{4.8}$$

Let K_h^* be the region bounded by the interface $\Gamma_K = \Gamma \cap K$ and the approximate line segment $\Gamma_{K,h}$. According to Assumption 3.1, each curve is of class C^2, then the area $|K_h^*| \lesssim h^3$. The polygon K_h^+ is an approximation to $K \cap \Omega^+$. It holds that

$$|(f^+, v_h^+)_{K_h^+} - (f^+, v_h^+)_{K\cap\Omega^+}| \leqslant \int_{K_h^*} |f^+ v_h^+| \,\mathrm{dx} \lesssim h \|f^+\|_{0,K_h^+} \|v_h^+\|_{0,K_h^+}. \tag{4.9}$$

A combination of (4.8) and (4.9) leads to

$$|(f^+, v_h^+)_{\Omega^+} - (f^+, v_h^+)_{\Omega^+,h}| \leqslant \sum_{K\cap\Omega^+\neq\emptyset} |(f^+, v_h^+)_{K\cap\Omega^+} - (f^+, v_h^+)_{K_h^+,h}| \lesssim h \|v_h^+\|_{\Omega^+,h}, \tag{4.10}$$

which leads to the estimate of the first term in the third inequality of (2.18). A similar analysis proves the second term in the third inequality and also the second inequality of (2.18).

By the definition of the bilinear form (2.5), the quadrature formula (4.1) and the integration by parts,

$$\begin{aligned} &a(\sigma^-, u^+; \tau_h^-, v_h^+) - a_h(\sigma^-, u^+; \tau_h^-, v_h^+) \\ =&\frac{1}{\beta^-}\left((\sigma^-, \tau_h^-)_{\Omega^-} - (\sigma^-, \tau_h^-)_{\Omega^-,h}\right) + \left((\beta^+\nabla u^+, \nabla v_h^+)_{\Omega^+} - (\beta^+\nabla u^+, \nabla v_h^+)_{\Omega^+,h}\right) \\ &- \left(\langle \tau_h^- \cdot \boldsymbol{n}, u^+\rangle_\Gamma - \langle \tau_h^- \cdot \boldsymbol{n}, u^+\rangle_{\Gamma,h}\right) + \left(\langle \sigma^- \cdot \boldsymbol{n}, v_h^+\rangle_\Gamma - \langle \sigma^- \cdot \boldsymbol{n}, v_h^+\rangle_{\Gamma,h}\right) \end{aligned} \tag{4.11}$$

For any element K intersecting with Γ, by a direct application of the integration by parts and the fact that $|K_h^*| \lesssim h^3$, it holds that

$$|\langle \tau_h^- \cdot \boldsymbol{n}, u^+\rangle_{\Gamma_K} - \langle \tau_h^- \cdot \boldsymbol{n}, u^+\rangle_{\Gamma_{K,h}}| = |\int_{K_h^*} u^+ \nabla\cdot \tau_h^- + \tau_h^- : \nabla u^+ \,\mathrm{dx}| \lesssim h(\|\nabla\cdot \tau_h^-\|_{0,K_h^-} + \|\tau_h^-\|_{0,K_h^-}).$$

A summation of the estimate above on all intersecting elements, together with the quadrature formula (3.3), gives

$$|\langle \tau_h^- \cdot \boldsymbol{n}, u^+\rangle_\Gamma - \langle \tau_h^- \cdot \boldsymbol{n}, u^+\rangle_{\Gamma,h}| \lesssim h \,|||\, (\tau_h^-, v_h^+) \,|||_{1,h}\,.$$

A similar analysis leads to $|\langle \sigma^- \cdot \boldsymbol{n}, v_h^+\rangle_\Gamma - \langle \sigma^- \cdot \boldsymbol{n}, v_h^+\rangle_{\Gamma,h}| \lesssim h \,|||\, (\tau_h^-, v_h^+)|||_{1,h}$, and also the last inequality of (2.18). By a similar analysis of (4.10), the summation of the first four terms on the right-hand side of (4.11) are also of $\mathcal{O}(h)$. A substitution of these estimates into (4.11) yields that

$$|a(\sigma^-, u^+; \tau_h^-, v_h^+) - a_h(\sigma^-, u^+; \tau_h^-, v_h^+)| \lesssim h \,|||\, (\tau_h^-, v_h^+)|||_{1,h}, \tag{4.12}$$

which proves the first inequality in (2.18). □

5 Numerical Examples

This section presents several numerical tests to illustrate the performance of the proposed DiFEM.

5.1 Example 1

Let the domain Ω be the square $(-2, 2)^2$, and the interface be a circle centered at the origin $(0, 0)$ with radius $r = 1.1$. Let $\mathcal{T}_0$ be the triangulation consisting of two right triangles obtained by cutting the unit square with a north-east line. Each triangulation $\mathcal{T}_i$ is refined into a half-sized triangulation uniformly, to get a higher level triangulation $\mathcal{T}_{i+1}$. Let $\mathcal{T}_2$ be the initial triangulation satisfying the requirement that the interface each edge at most once, which is depicted in Figure 3(a).

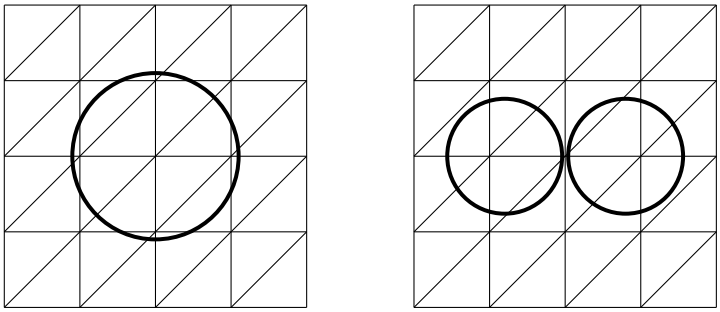

Figure 3 The interfaces in Example 1(left) and Example 2(right).

Let Ω^- be the region enclosed by the circle, and Ω^+ be the region outside the circle. Consider the interface problem (1.1) with $\beta^+ = 1$ and various β^-, and the right-hand side f and the boundary condition g are computed such that the exact solution

$$u = \begin{cases} e^{x^2+y^2-r^2} + \beta^- r^2 - 1 & \text{if } x^2+y^2 \leqslant r^2 \\ \beta^-(x^2+y^2) & \text{if } x^2+y^2 > r^2 \end{cases}$$

satisfying the continuity conditions in (1.1).

Table 1 - 5 record the relative errors $\|\nabla(u^+ - u_h^+)\|_{0,\Omega_h^+}$, $\|u^+ - u_h^+\|_{0,\Omega_h^+}$, $\|\sigma^- - \sigma_h^-\|_{0,\Omega_h^-}$ and $\|u^- - u_h^-\|_{0,\Omega_h^-}$, and the convergence rate of solutions by the DiFEM when $\beta^- = 10^{-3}$, 10^{-1}, 1, 10 and 10^3, respectively. These results coincide with the convergence result in Theorem 3.2, and the convergence rate does not deteriorate even the ratios $\frac{\beta^-}{\beta^+}$ or $\frac{\beta^+}{\beta^-}$ are large, which verifies the efficiency of the proposed DiFEM. It is pointed out in [30] that it is inappropriate to use conforming finite element methods for large jump-coefficient problems because of the coefficient-dependent error estimate bound. For the DiFEM (2.12) coupling the conforming finite element method and the mixed finite element method, it shows surprisedly that the convergence rate of $\|\sigma^- - \sigma_h^-\|_{0,\Omega_h^-}$ and $\|u^- - u_h^-\|_{0,\Omega_h^-}$ on Ω^- are even higher than one when the ratio $\frac{\beta^-}{\beta^+}$ is relatively large as indicated in Table 5, while $\|\nabla(u^+ - u_h^+)\|_{0,\Omega_h^+}$ on Ω^+ remains of accuracy $\mathcal{O}(h)$.

Table 1 Relative errors and convergence rates for Example 1 with $\frac{\beta^-}{\beta^+} = 0.001$.

	$\|\nabla(u^+ - u_h^+)\|_{0,\Omega_h^+}$	rate	$\|u^+ - u_h^+\|_{0,\Omega_h^+}$	rate	$\|\sigma^- - \sigma_h^-\|_{0,\Omega_h^-}$	rate	$\|u^- - u_h^-\|_{0,\Omega_h^-}$	rate
$\mathcal{T}_2$	3.99E-03		1.09E-04		4.65E-01		1.01E+00	
$\mathcal{T}_3$	1.43E-03	1.48	4.95E-04	-2.18	2.93E-01	0.67	9.69E-01	0.05
$\mathcal{T}_4$	6.97E-04	1.04	3.86E-04	0.36	2.11E-01	0.47	4.39E-01	1.14
$\mathcal{T}_5$	3.31E-04	1.07	9.43E-05	2.03	1.10E-01	0.94	1.88E-01	1.22
$\mathcal{T}_6$	1.64E-04	1.01	2.35E-05	2.00	5.87E-02	0.91	8.00E-02	1.23
$\mathcal{T}_7$	8.20E-05	1.00	6.01E-06	1.97	2.98E-02	0.98	3.76E-02	1.09

5.2 Example 2

This example tests the effectivity of the proposed DiFEM for (2.12) on the unit square $(0,1)^2$ with multiple interfaces as depicted in Figure 3(right). In this case, the interface is the union of two closely located circles with radius $r = 0.19$ and centers $(0.3, 0.5)$ and $(0.7, 0.5)$, respectively. Let Ω^- be the region enclosed by the two circles and Ω^+ be the region outside the circles. Compute the right-hand side f and

Table 2 Relative errors and convergence rates for Example 1 with $\frac{\beta^-}{\beta^+} = 0.1$.

	$\|\nabla(u^+ - u_h^+)\|_{0,\Omega_h^+}$	rate	$\|u^+ - u_h^+\|_{0,\Omega_h^+}$	rate	$\|\sigma^- - \sigma_h^-\|_{0,\Omega_h^-}$	rate	$\|u^- - u_h^-\|_{0,\Omega_h^-}$	rate
$\mathcal{T}_2$	3.10E-01		1.09E-02		3.40E-01		1.00E+00	
$\mathcal{T}_3$	1.21E-01	1.35	4.47E-02	-2.04	2.47E-01	0.46	8.74E-01	0.20
$\mathcal{T}_4$	5.93E-02	1.03	2.48E-02	0.85	1.79E-01	0.47	2.80E-01	1.64
$\mathcal{T}_5$	2.85E-02	1.06	5.92E-03	2.06	9.51E-02	0.91	1.18E-01	1.25
$\mathcal{T}_6$	1.42E-02	1.01	1.47E-03	2.01	5.07E-02	0.91	5.03E-02	1.23
$\mathcal{T}_7$	7.08E-03	1.00	3.77E-04	1.97	2.58E-02	0.98	2.37E-02	1.09

Table 3 Relative errors and convergence rates for Example 1 with $\frac{\beta^-}{\beta^+} = 1$.

	$\|\nabla(u^+ - u_h^+)\|_{0,\Omega_h^+}$	rate	$\|u^+ - u_h^+\|_{0,\Omega_h^+}$	rate	$\|\sigma^- - \sigma_h^-\|_{0,\Omega_h^-}$	rate	$\|u^- - u_h^-\|_{0,\Omega_h^-}$	rate
$\mathcal{T}_2$	2.24E-01		9.77E-02		4.75E-02		1.88E-01	
$\mathcal{T}_3$	1.12E-01	1.00	2.88E-02	1.76	3.34E-02	0.51	3.16E-02	2.57
$\mathcal{T}_4$	5.55E-02	1.01	6.71E-03	2.10	1.86E-02	0.85	1.31E-02	1.28
$\mathcal{T}_5$	2.77E-02	1.00	1.66E-03	2.02	9.92E-03	0.90	5.66E-03	1.21
$\mathcal{T}_6$	1.38E-02	1.00	4.24E-04	1.97	5.04E-03	0.98	2.68E-03	1.08

Table 4 Relative errors and convergence rates for Example 1 with $\frac{\beta^-}{\beta^+} = 10$.

	$\|\nabla(u^+ - u_h^+)\|_{0,\Omega_h^+}$	rate	$\|u^+ - u_h^+\|_{0,\Omega_h^+}$	rate	$\|\sigma^- - \sigma_h^-\|_{0,\Omega_h^-}$	rate	$\|u^- - u_h^-\|_{0,\Omega_h^-}$	rate
$\mathcal{T}_2$	4.96E-01		3.47E-01		5.73E-02		3.05E-01	
$\mathcal{T}_3$	2.26E-01	1.13	9.88E-02	1.81	1.12E-02	2.36	3.51E-02	3.12
$\mathcal{T}_4$	1.13E-01	1.00	2.87E-02	1.78	3.72E-03	1.59	9.40E-03	1.90
$\mathcal{T}_5$	5.63E-02	1.01	6.65E-03	2.11	2.16E-03	0.78	2.26E-03	2.06
$\mathcal{T}_6$	2.81E-02	1.00	1.63E-03	2.02	1.07E-03	1.01	6.93E-04	1.70
$\mathcal{T}_7$	1.40E-02	1.00	4.17E-04	1.97	5.20E-04	1.05	2.85E-04	1.28

Table 5 Relative errors and convergence rates for Example 1 with $\frac{\beta^-}{\beta^+} = 1000$.

	$\|\nabla(u^+ - u_h^+)\|_{0,\Omega_h^+}$	rate	$\|u^+ - u_h^+\|_{0,\Omega_h^+}$	rate	$\|\sigma^- - \sigma_h^-\|_{0,\Omega_h^-}$	rate	$\|u^- - u_h^-\|_{0,\Omega_h^-}$	rate
$\mathcal{T}_2$	8.56E-01		2.70E-01		7.81E-03		1.67E-01	
$\mathcal{T}_3$	2.38E-01	1.85	9.65E-02	1.48	1.25E-03	2.65	4.25E-02	1.98
$\mathcal{T}_4$	1.14E-01	1.06	2.89E-02	1.74	1.95E-04	2.68	9.62E-03	2.15
$\mathcal{T}_5$	5.74E-02	0.99	7.01E-03	2.05	5.78E-04	-1.57	3.02E-03	1.67
$\mathcal{T}_6$	2.84E-02	1.02	1.66E-03	2.08	9.84E-05	2.55	5.55E-04	2.44
$\mathcal{T}_7$	1.41E-02	1.01	4.18E-04	1.99	3.47E-05	1.50	1.32E-04	2.07

the boundary condition g with $\beta^+ = 1$ such that the exact solution

$$u = \begin{cases} \dfrac{1}{\beta^-}\phi(x) & \text{if } x \in \Omega^- \\ \phi(x) & \text{if } x \in \Omega^+ \end{cases},$$

where $\phi(x) = ((x-0.3)^2 + (y-0.5)^2 - r^2)((x-0.7)^2 + (y-0.5)^2 - r^2)$. Take the same triangulation as in Example 1 and let $\mathcal{T}_2$ be the initial triangulation.

Table 6 - 7 record the relative errors $\|\nabla(u^+ - u_h^+)\|_{0,\Omega_h^+}$, $\|u^+ - u_h^+\|_{0,\Omega_h^+}$, $\|\sigma^- - \sigma_h^-\|_{0,\Omega_h^-}$ and $\|u^- -$

$u_h^-\|_{0,\Omega_h^-}$, and the convergence rate of solutions by the DiFEM when $\beta^- = 1$ and 100, respectively. It shows that the proposed DiFEM is effective even when the interface is the union of closely located curves. The results in Table 6 - 7 coincide with the convergence result in Theorem 3.2, and the convergence rate does not deteriorate even the ratios $\frac{\beta^-}{\beta^+}$ or $\frac{\beta^+}{\beta^-}$ are large.

Table 6 Relative errors and convergence rates for Example 2 with $\frac{\beta^-}{\beta^+} = 1$.

	$\|\nabla(u^+ - u_h^+)\|_{0,\Omega_h^+}$	rate	$\|u^+ - u_h^+\|_{0,\Omega_h^+}$	rate	$\|\sigma^- - \sigma_h^-\|_{0,\Omega_h^-}$	rate	$\|u^- - u_h^-\|_{0,\Omega_h^-}$	rate
$\mathcal{T}_2$	4.66E-01		3.16E-01		6.16E-02		7.30E-02	
$\mathcal{T}_3$	2.44E-01	0.94	8.45E-02	1.90	1.86E-02	1.72	2.62E-02	1.48
$\mathcal{T}_4$	1.23E-01	0.98	2.14E-02	1.98	8.90E-03	1.07	9.26E-03	1.50
$\mathcal{T}_5$	6.18E-02	1.00	5.38E-03	1.99	4.53E-03	0.97	3.95E-03	1.23
$\mathcal{T}_6$	3.09E-02	1.00	1.35E-03	2.00	2.31E-03	0.97	1.81E-03	1.13

Table 7 Relative errors and convergence rates for Example 2 with $\frac{\beta^-}{\beta^+} = 100$.

	$\|\nabla(u^+ - u_h^+)\|_{0,\Omega_h^+}$	rate	$\|u^+ - u_h^+\|_{0,\Omega_h^+}$	rate	$\|\sigma^- - \sigma_h^-\|_{0,\Omega_h^-}$	rate	$\|u^- - u_h^-\|_{0,\Omega_h^-}$	rate
$\mathcal{T}_2$	5.01E-01		3.95E-01		7.35E-03		5.06E-02	
$\mathcal{T}_3$	2.45E-01	1.03	8.48E-02	2.22	2.44E-03	1.59	2.25E-03	4.49
$\mathcal{T}_4$	1.23E-01	0.99	2.16E-02	1.98	4.55E-04	2.42	1.43E-03	0.65
$\mathcal{T}_5$	6.19E-02	1.00	5.41E-03	2.00	1.27E-04	1.84	4.72E-04	1.60
$\mathcal{T}_6$	3.10E-02	1.00	1.35E-03	2.00	5.61E-05	1.18	1.34E-04	1.82

5.3 Example 3

This example tests the effectivity of the proposed DiFEM for (2.12) on the square $(-1,1)^2$ with the interface being a flower, where the corresponding level set function is defined as

$$r = \frac{1}{2} - 2^{\sin(5\theta)-3}.$$

Let $\Omega^+ = \{(r,\theta) : r > \frac{1}{2} - 2^{\sin(5\theta)-3}\}$ and $\Omega^- = \{(r,\theta) : r < \frac{1}{2} - 2^{\sin(5\theta)-3}\}$. Compute the right-hand side f and the boundary condition g such that the exact solution

$$u(r,\theta) = \begin{cases} \frac{1}{\beta^-} r^2 (r - \frac{1}{2} + 2^{\sin(5\theta)-3}) & \text{if } (r,\theta) \in \Omega^-, \\ \frac{1}{\beta^+} r^2 (r - \frac{1}{2} + 2^{\sin(5\theta)-3}) & \text{if } (r,\theta) \in \Omega^+ \end{cases}, \tag{5.1}$$

Take the same triangulation as in Example 1 and let $\mathcal{T}_1$ be the initial triangulation.

As shown in Figure 4, the region enclosed by the interface is no longer convex. Table 8 - 9 record the relative errors $\|\nabla(u^+ - u_h^+)\|_{0,\Omega_h^+}$, $\|u^+ - u_h^+\|_{0,\Omega_h^+}$, $\|\sigma^- - \sigma_h^-\|_{0,\Omega_h^-}$ and $\|u^- - u_h^-\|_{0,\Omega_h^-}$, and the convergence rate of solutions by the direct finite element method when $\beta^- = 1$ and 10, respectively. The results in Table 8 - 9 also verify the convergence result in Theorem 3.2.

References

1 Ivo Babuska. The finite element method for elliptic equations with discontinuous coefficients. *Computing*, 5:207–213, 1970.

2 Nelly Barrau. Généralisation de la méthode nitsche xfem pour la discrétisation de problèmes d'interface elliptiques. (nxfem generalization for elliptic interface problems discretization). 2013.

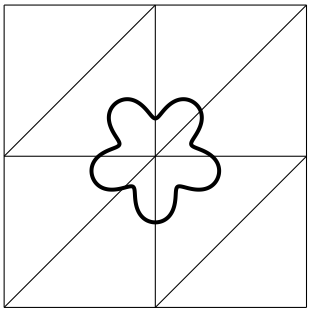

Figure 4 The interface for Example 3.

Table 8 Relative errors and convergence rates for Example 3 with $\frac{\beta^-}{\beta^+} = 1$.

	$\|\nabla(u^+ - u_h^+)\|_{0,\Omega_h^+}$	rate	$\|u^+ - u_h^+\|_{0,\Omega_h^+}$	rate	$\|\sigma^- - \sigma_h^-\|_{0,\Omega_h^-}$	rate	$\|u^- - u_h^-\|_{0,\Omega_h^-}$	rate
$\mathcal{T}_1$	3.89E-01		2.27E-01		2.24E-02		2.31E-02	
$\mathcal{T}_2$	2.02E-01	0.95	5.92E-02	1.94	1.76E-02	0.35	1.04E-02	1.16
$\mathcal{T}_3$	1.03E-01	0.97	1.60E-02	1.89	9.09E-03	0.95	2.66E-03	1.96
$\mathcal{T}_4$	5.17E-02	0.99	3.84E-03	2.06	4.50E-03	1.01	1.24E-03	1.10
$\mathcal{T}_5$	2.59E-02	1.00	9.63E-04	1.99	2.22E-03	1.02	5.16E-04	1.26

Table 9 Relative errors and convergence rates for Example 3 with $\frac{\beta^-}{\beta^+} = 10$.

	$\|\nabla(u^+ - u_h^+)\|_{0,\Omega_h^+}$	rate	$\|u^+ - u_h^+\|_{0,\Omega_h^+}$	rate	$\|\sigma^- - \sigma_h^-\|_{0,\Omega_h^-}$	rate	$\|u^- - u_h^-\|_{0,\Omega_h^-}$	rate
$\mathcal{T}_1$	3.89E-01		2.26E-01		1.13E-02		1.19E-02	
$\mathcal{T}_2$	2.02E-01	0.95	5.87E-02	1.95	5.80E-03	0.97	2.24E-03	2.41
$\mathcal{T}_3$	1.03E-01	0.97	1.56E-02	1.91	1.24E-03	2.23	3.43E-04	2.71
$\mathcal{T}_4$	5.17E-02	0.99	3.83E-03	2.02	5.26E-04	1.23	2.55E-04	0.43
$\mathcal{T}_5$	2.59E-02	1.00	9.61E-04	1.99	2.41E-04	1.13	7.86E-05	1.70

3 John W. Barrett and Charles M. Elliott. Fitted and unfitted finite-element methods for elliptic equations with smooth interfaces. *Ima Journal of Numerical Analysis*, 7:283–300, 1987.

4 Daniele Boffi, Franco Brezzi, and Michel Fortin. Mixed finite element methods and applications. 2013.

5 Erik Burman, Susanne Claus, Peter Hansbo, Mats G. Larson, and André Massing. Cutfem: Discretizing geometry and partial differential equations. *International Journal for Numerical Methods in Engineering*, 104:472 – 501, 2015.

6 Erik Burman, Johnny Guzmán, Manuel A. Sánchez, and Marcus V. Sarkis. Robust flux error estimation of an unfitted nitsche method for high-contrast interface problems. *arXiv: Numerical Analysis*, 2016.

7 Erik Burman and Peter Hansbo. Fictitious domain finite element methods using cut elements: I. a stabilized lagrange multiplier method. *Computer Methods in Applied Mechanics and Engineering*, 199:2680–2686, 2010.

8 Erik Burman and Peter Hansbo. Fictitious domain finite element methods using cut elements. *Applied Numerical Mathematics*, 62:328–341, 2012.

9 Raffael Casagrande, Christoph Winkelmann, Ralf Hiptmair, and J. Ostrowski. Dg treatment of non-conforming interfaces in 3d curl-curl problems. 2016.

10 Long Chen, Huayi Wei, and Min Wen. An interface-fitted mesh generator and virtual element methods for elliptic interface problems. *J. Comput. Phys.*, 334:327–348, 2017.

11 Zhiming Chen, Yuanming Xiao, and Linbo Zhang. The adaptive immersed interface finite element method for elliptic and maxwell interface problems. *J. Comput. Phys.*, 228:5000–5019, 2009.

12 Zhiming Chen and Jun Zou. Finite element methods and their convergence for elliptic and parabolic interface problems. *Numerische Mathematik*, 79:175–202, 1998.

13 Philippe G. Ciarlet. The finite element method for elliptic problems. In *Classics in applied mathematics*, 2002.

14 Charles M. Elliott and Thomas Ranner. Finite element analysis for a coupled bulk-surface partial differential equation. *Ima Journal of Numerical Analysis*, 33:377–402, 2013.

15 Yanpeng Gong, Bo Li, and Zhilin Li. Immersed-interface finite-element methods for elliptic interface problems with nonhomogeneous jump conditions. *SIAM J. Numer. Anal.*, 46:472–495, 2007.

16 Yanpeng Gong and Zhilin Li. Immersed interface finite element methods for elasticity interface problems with non-homogeneous jump conditions. *Numerical Mathematics-theory Methods and Applications*, 2009.

17 Grégory Guyomarc'h, Chang-Ock Lee, and Kiwan Jeon. A discontinuous galerkin method for elliptic interface problems with application to electroporation. *Communications in Numerical Methods in Engineering*, 25:991–1008, 2009.

18 Anita Hansbo and Peter Hansbo. An unfitted finite element method, based on nitsche's method, for elliptic interface problems. *Computer Methods in Applied Mechanics and Engineering*, 191:5537–5552, 2002.

19 Anita Hansbo and Peter Hansbo. A finite element method for the simulation of strong and weak discontinuities in solid mechanics. *Computer Methods in Applied Mechanics and Engineering*, 193:3523–3540, 2004.

20 Lisa Huynh, Ngoc Cuong Nguyen, Jaime Peraire, and Boo Cheong Khoo. A high-order hybridizable discontinuous galerkin method for elliptic interface problems. *International Journal for Numerical Methods in Engineering*, 93, 2013.

21 Zhilin Li and Kazufumi Ito. The immersed interface method: Numerical solutions of pdes involving interfaces and irregular domains (frontiers in applied mathematics). 2006.

22 Zhilin Li, Tao Lin, and Xiao hui Wu. New cartesian grid methods for interface problems using the finite element formulation. *Numerische Mathematik*, 96:61–98, 2003.

23 Johannes C. C. Nitsche. Über ein variationsprinzip zur lösung von dirichlet-problemen bei verwendung von teilräumen, die keinen randbedingungen unterworfen sind. *Abhandlungen aus dem Mathematischen Seminar der Universität Hamburg*, 36:9–15, 1971.

24 P.-A. Raviart and J. M. Thomas. A mixed finite element method for 2nd order elliptic problems. In *Mathematical aspects of finite element methods (Proc. Conf., Consiglio Naz. delle Ricerche (C.N.R.), Rome, 1975)*,, Lecture Notes in Math., Vol. 606,, pages 292–315. ,, 1977.

25 Bo Wang and Boo Cheong Khoo. Hybridizable discontinuous galerkin method (hdg) for stokes interface flow. *J. Comput. Phys.*, 247:262–278, 2013.

26 Haimei Wang, Feng Wang, Jinru Chen, and Haifeng Ji. A conforming virtual element method based on unfitted meshes for the elliptic interface problem. *Journal of Scientific Computing*, 96:1–32, 2023.

27 Qiuliang Wang and Jinru Chen. An unfitted discontinuous galerkin method for elliptic interface problems. *J. Appl. Math.*, 2014:241890:1–241890:9, 2014.

28 T. Warburton and J.S. Hesthaven. On the constants in hp-finite element trace inverse inequalities. *Computer Methods in Applied Mechanics and Engineering*, 192(25):2765–2773, 2003.

29 Jinchao Xu. Estimate of the convergence rate of finite element solutions to elliptic equations of second order with discontinuous coefficients. *Natur. Sci. J. Xiangtan Univ.*, 1:1–5, 1982.

30 Shangyou Zhang. Coefficient jump-independent approximation of the conforming and nonconforming finite element solutions. *Advances in Applied Mathematics and Mechanics*, 8:722–736, 2016.